ScienSage

Journal of Advanced Scientific Research

Available online through http://www.sciensage.info

ISSN
0976-9595
Review Article

PURIFICATION OF WASTEWATER THROUGH PHOTOCATALYTIC DEGRADATION OF POLLUTANTS USING PZT AND ITS COMPOSITES

T. K. Mandal*[1], Vipin Patait[2]

[1]*ICFAI Tech School, ICFAI University, Rajawala Road, Selaqui, Dehradun, Uttarakhand, India*

[2]*Samrat Ashok Technological Institute, Vidisha, Madhya Pradesh, India*

**Corresponding author: dr.mandal@iudehradun.edu.in*

ABSTRACT

Lead zirconate titanate (PZT) and its composite ferroelectric materials have been studied for the application in purification of waste water containing organic dyes. The recent reports on PZT by different researchers for the photocatalytic application in the degradation of orgnic dyes have been reviewed. Synthesis, characterization and properties of as prepared PZT materials by different authors have been reviewed. The present status of photodegradation activity of PZT and similar ferroelectric materials and the strategy for enhancement of photocatalytic performance by different researchers has also been studied.

Keywords: PZT, Ferroelectrics, Photocatalysis, Piezocatalysis, Piezophotocatalysis.

1. INTRODUCTION

The discharge of industrial effluents having organic pollutants has become a great issue at present days since the freshwater resource of the earth is deteriorating because of presence of these pollutants. A number of efforts such as filtration, biological treatment, sorption processes and catalytic oxidation have been employed for the treatment of industrial effluent and waste water [1]. Actually, the toxic pollutants should be converted to non-toxic species through an environment friendly method [2]. Photocatalytic degradation of organic pollutants using ferroelectric PZT and compounds with similar properties, utilizing solar energy, is a novel approach to solve the problem [3-4]. Although several workers are involved on the research of oxide photoctalysts, the enhancement of efficiency of photo-catalysis is still a challenge among the researchers.

Various materials and processes like surface decoration by noble metal nanoparticles, engineering of band-gaps, preparing heterojunction between two semiconductors with appropriate band gaps have been applied [5-7]. Unfortunately no reasonable development has been achieved for this. A new approach for the development of photocatalyic activity has been observed with the ferroelectric materials. These materials have been considered as wide band gap semiconductors for a period of time [8]. Ferroelectric materials possess a spontaneous polarisation originating as the result of the displacement of the centre of the charges in a unit cell [9]. Macroscopic charges will be induced by this spontaneous polarisation on the surface of ferro-electrics. Because of this the internal depolarisation field will force the charge carriers to flow in reverse directions, creating in spatial separation of oxidation and reduction reactions [10-12]. The charge on the surface will be compensated by free charge carriers and defects in the ferroelectric bulk and the adsorbed charged molecules from the environment [13-14]. Also, the spontaneous polarisation of ferroelectric materials will have interactions with the dipoles of adsorbed molecules. This decreases the energy requirement for breaking the bonds [15-16]. Thus, ferroelectric materials can be better applied in photocatalysis.

Because of possessing ferroelectric properties, PZT has also valuable applications in nonvolatile memories, ultrasonic sensors, actuators and infrared detectors [17-28]. Solid solutions of PZT exhibit the morphotropic phase boundary (MPB) that divides PZT structures into rhombohedral and tetragonal regions [9]. A rhombo-hedral Zr-rich phase is separated from a tetragonal Ti-rich phase in MPB. In MPB region, the dielectric constant, piezoelectric constant as well as electro-mechanical coupling coefficients are at maximum value [9, 28]. The MPB in $PbZr_xTi_{1-x}O_3$ ($0 \leq x \leq 1$) exists at around $x=0.5$ [9]. Development of processing methods that produce PZT material with fine particle size and

high chemical homogeneity is very challenging as both these features are necessary to prepare PZT powders with required microstructures like grain size, grain morphology and grain distribution [18]. These micro-structural paprameters govern the important role in determining the polarization values.

The objective of the present investigation is to study the applications of PZT and its composites in photocatalytic degradation of pollutants, present in the wastewater. The structure and properties of PZT responsible for the application in photodegradation is demonstrated briefly. A comparative study of synthesis, characterization and properties of PZT by different workers has been presented. The photocatalytic performance of PZT and similar ferroelectric materials and the means for increment of photodegradation activity of these materials by different workers has also been addressed.

2. PREPARATION AND CHARACTERIZATION OF PZT MATERIALS

PZT ceramics have been prepared traditionally employing solid-state reaction routes, using oxide mixtures at high temperatures [25]. But, to overcome the presence of chemical inhomogeneities and fluctuation in compositions in the PZT ceramics, synthesized from oxide mixtures, many new approaches have been established. Zeng et al [21] used sol-gel process for the preparation of $PbZr_{0.5}Ti_{0.5}O_3$ thin films. Sol-gel method was also employed by Wu et al [22] to prepare $PbZr_{0.52}Ti_{0.48}O_3$ powders with the size in submicrometer ranges. Surowiak et al [20] explored sol-gel method to prepare $PbZr_{0.5}Ti_{0.5}O_3$ particles with average size of around 30 nm. Lead lanthanum zirconate titanate $[(Pb_{0.92}La_{0.08})\ (Zr_{0.60}TiO_{0.40})O_3]$ (PLZT) was synthesized using the sol-gel method by James et al [32]. X-ray diffraction (XRD) study exhibited the perovskite structure of PLZT at room temperature with an average size of 30 nm. The as prepared materials were also characterized by small angle X-ray scattering (SAXS), Scanning electron microscopic (SEM) studies, TG-DTA and DSC analysis. Although, sol-gel method is used by several workers, some limitations of this method have been pointed out by the researchers [21-23]. To overcome this problem, polymer precursor method has been utilized by Mandal and co-workers to synthesize defect-free PZT materials with uniform particle size [18-22, 25]. Peng et al [33] studied the microstructure, dielectric, ferroelectric, ferromagnetic and magneto-electric (ME) coupling properties of PZT-CFO composites. The ME composites were prepared by them applying hydrothermal method and ceramic sintering process. Wang et al [34] fabricated $Pb(Zr,Ti)O_3$ fibers through hydrothermal method and the as prepared PZT material's phase, composition and orientation was characterized by Raman spectroscopy. The submicron PZT fibers were exhibited to have tetragonal pervoskite phase. The existence of spontaneous polarization was also confirmed with the material. $PbZr_{0.3}Ti_{0.7}O_3$ thick films and detectors were prepared by Wu et al [35] for the pyroelectric applications. The films have been fabricated on alumina substrates by screen-printing technology. The permittivity and loss tangent of the thick films were 94 and 0.017, respectively. Curie temperature of PZT thick film was 425°C.

The phase formation and structure of the as prepared PZT materials have been analysed by XRD. Crystallite size has been calculated applying Scherrer's formula [25]. The particle size and surface morphology of the formed particles have been estimated utilizing TEM and SEM respectively. Surface area of the as synthesized materials has been determined exploring BET measurements. The dielectric constant and Curie temperature of the samples were investigated with the help of an inductance-capacitance-resistance meter. Different preparation methods and properties of the as prepared PZT materials have been summarized in Table 1.

Table 1: Preparation methods and properties of as prepared PZT materials by different workers

Material	Preparation Method	Properties	Ref.
$PbZr_{0.5}Ti_{0.5}O_3$ powder	Sol-gel	Particle size: submicrometer	[30]
$PbZr_{0.5}Ti_{0.5}O_3$ particles	Sol-gel	Particle size: 30 nm	[31]
$[(Pb_{0.92}La_{0.08})\ (Zr_{0.60}TiO_{0.40})O_3$	Sol-gel	Particle size: 30 nm Structure: perovskite	[32]
$PbZr_{0.7}Ti_{0.3}O_3$ nanoparticles	Polymer precursor	Crystal symmetry: tetragonal; Particle size: 25 nm, Specific surface area = 49 m^2/g.	[18]
$PbZr_{0.52}Ti_{0.48}O_3$ Fibrils	Polymer precursor	Crystal symmetry: orthorhombic; Lattice parameters: a = 0.4038 nm b = 0.4017 and c = 0.4148 nm; Ferroelectric, T_C = 370°C	[21]

$PbZr_{0.5}Ti_{0.5}O_3$ ceramics	Polymer precursor	Crystal symmetry: mixture of tetragonal (P4mm) and hexagonal (R3c); Particle size: 27 nm; Ferroelectric: ε_{max} = 25000 with ε = 1100 at room temperature at 1 kHz; Specific surface area = 34 m^2/g.	[25]
(1- x)$Pb(Zr_{0.52}Ti_{0.48})O_3$-(x)$CoFe_2O_4$ (PZT-CFO) (x = 0.20, 0.35,and0.50) magnetoelectric composites	Hydrothermal synthesis and ceramic sintering process	Multiferroics (both ferroelectric and ferromagnetic properties coexist in the ME composites prepared), Saturation magnetization, Ms (emu/g): 22.8 (@PZT:CFO = 50:50), Remanent magnetization, Mr (emu/g): 6.95 (@PZT:CFO = 50:50)	[33]
$Pb(Zr,Ti)O_3$ fibers	Hydrothermal	Structure: tetragonal pervoskite, ferroelectric	[34]
$PbZr_{0.3}Ti_{0.7}O_3$ thick films	Screen-printing technology	Film property-permittivity: 94; loss tangent: 0.017; T_C: 425°C. Application: pyroelectric	[35]
PZT (Zr:Ti = 0.5:0.5) powder	Molten salt synthesis	Particle size: submicron range Application: ink jet printing	[36]
$Pb(Zr_{0.3}Ti_{0.7})O_3$ films	Chemical solution deposition	Crystal symmetry: Tetragonal, Pr values of 34 $\mu C/cm^2$	[37]

3. PHOTOCATALYTIC DEGRADATION OF PZT COMPOSITES AND RELATED FERRO-ELECTRICS

The material synthesized using PZT/ TiO_2 nanoparticles prepared by Wu et al [38] showed effective photo-catalytic degradation activity with Rhodamine B in visible light irradiation. $Pb(Zr_{0.52}Ti_{0.48})O_3/TiO_2$ composite nanostructured heterojunction was synthesized by Huang et al [39] applying sol-gel process. Synthesized material was characterized by XRD, BET, TEM, UV-vis, electrochemistry and spin-trapping EPR. Photo-catalytic performances of the as prepared composite were examined by them decomposing ethylene in gas phase. Excellent photocatalytic activity in UV light or simulated sunlight irradiation was exhibited by Pb $(Zr_{0.52}Ti_{0.48})O_3/TiO_2$ composite. A plausible mechanism for photocatalytic activity of $Pb(Zr_{0.52}Ti_{0.48})O_3/TiO_2$ was proposed by the authors. The photocatalytic performance of TiO_2 nanotubes prepared by hydro-thermal method was evaluated by degradation of methyl orange by Lai et al [40]. As prepared, TiO_2 nanotubes showed superior photocatalytic oxidation rate (78% degradation) in UV light in 5h, because of the available high active surface area to form more hydroxyl radicals (·OH) required for triggering photocatalytic oxidation reactions. You et al [41] explored hydrothermal route to prepare Piezoelectric-ZnO@photoelectric-TiO_2 core-shell nanofibers and they employed it to photo-degrade Methyl Orange. The as prepared ZnO@TiO_2 core-shell nanofibers are of high efficiency and non-toxic for the treatment of dye wastewater. The application of piezoelectric materials in photocatalysis and piezoelectric-catalysis in environmental purification has been investigated by Liang et al [42]. In order to prevent photoelectron-hole recombination Feng at al [43] introduced a piezoelectric field increasing the photocatalytic performance. But, additional mechanical force is required for the formation of a piezoelectric field. To overcome this problem, Feng at al [43] worked to design the catalyst that harvests the discrete energy like the fluid mechanical energy to create the electric field. For that, Feng at al [43] fabricated PZT/TiO_2 core-shell configured composite, applying a coating method. An internal piezoelectric field was generated by them with the mechanical energy of water. The photocatalytic decomposition rate of RhB, BPA, phenol, p-chlorophenol was improved largely in their research. This was because of the effect of piezoelectric field produced directly from generating the discrete fluid mechanical energy. $Ba_{0.875}Ca_{0.125}Ti_{0.95}Sn_{0.05}O_3$ (BCT-Sn) material was investigated for photocatalytic, piezocatalytic and piezo-photocatalytic effects by Qifeng et al [44] by poling the material through corona poling. They found that poling induces valuable impact on photocatalytic activity. The poled material was able to degrade Methylene blue effectively through piezocatalysis. The authors also examined the material for piezo-photocatalytic (piezocatalysis + photo-catalysis) effect. Piezotronics enhanced photocatalytic activities of Ag-$BaTiO_3$ plasmonic photocatalysts' was

studied by Shuya et al [45]. The prepared the Ag-$BaTiO_3$ material by precipitating Ag nanoparticles on $BaTiO_3$ nano-piezoelectric applying a photochemical reducing process. Ag-$BaTiO_3$ material exhibited a high photo-catalytic activity of degrading 83% Rhodamin B in 75 min in full-spectrum of light in ultrasonic excitation. Their work shows an effective technique for the environmental purification and the idea can be extended to other piezoelectric materials. Shenyu et al [46] found the increased photodegradation of trimethoxy-pyrimidine (TMP) was exhibited through the piezo-photocatalysis of barium titanate/silver orthophosphate ($BaTiO_3/Ag_3PO_4$) exploring mechanical vibration and visible light energy simultaneously [46]. A facile co-precipitation method was used by them to prepare the hybrid $BaTiO_3/Ag_3PO_4$. In their investigation, the efficiency of the removal of TMP by the piezo-photocatalysis of $BaTiO_3/Ag_3PO_4$ was increased to 85% in 30 min time. Their study showed that the piezoelectric field generated from the $BaTiO_3$ enhanced the separation of electron-hole of Ag_3PO_4, generating more holes to decompose TMP. This enhancement of photo-generated electron-hole separation and for capturing mechanical and visible energy from the environment is a good strategy. The role of polarization in photocatalysis has been addressed by Chen et al [47]. Polarization is an effective strategy to overcome the problem of rapid recombination of charge carriers in the bulk phase and on the surface of photocatalysts and thus effectively enhancing photocatalysis activity. Abhinay et al [48] prepared the heterojunction $(Ba_{0.85}Ca_{0.15})$ $(Zr_{0.1}Ti_{0.9})TiO_3$(BCZT)/Bi_2O_3 composites with solid-state process. As-prepared composites were charac-terized by them through UV-vis, XRD, EDX, SEM and PL spectroscopy. They applied the as prepared material for photocatalysis degradation on rhodamine B in UV-vis light. They observed that the heterojunction com-posites of BCZT/Bi_2O_3 exhibit superior photocatalytic activity in compare to BCZT or Bi_2O_3. BCZT/Bi_2O_3 (50:50) composite showed a lower recombination rate of electron-hole pair and exhibited the maximum photocatalytic performance. Photocatalytic applications of PZT composites and related ferroelectrics are summarized in Table 2.

Table 2: Photocatalytic applications of PZT composites and related ferroelectrics

Material	Preparation method	Application	Ref.
PZT/TiO_2 NPs		photocatalytic activity for degradation of Rhodamine B	[38]
$Pb(Zr_{0.52}Ti_{0.48})O_3/TiO_2$ composite nanostructured heterojunction	Sol-gel method	Photocatalyst	[39]
TiO_2	Hydrothermal method	TiO_2 nanotubes were used for photocatalytic degradation of methyl orange dye	[40]
ZnO@photoelectric-TiO_2 core-shell nanofibers	Hydrothermal method	used for photocatalytic degradation of methyl orange	[41]
PZT/TiO_2 core-shell configuration	Coating method	Improved photocatalysis in RhB, BPA, phenol, p-chlorophenol	[43]
$Ba_{0.875}Ca_{0.125}Ti_{0.95}Sn_{0.05}O_3$ (BCT-Sn)	-	BCT-Sn showed piezo-photocatalytic effect on methylene blue	[44]
Ag-$BaTiO_3$	Photochemical reducing approach	piezo-photocatalysts	[45]
$BaTiO_3/Ag_3PO_4$ hybrid	Facile co-precipitation method	enhanced photodegradation of trimethoxypyrimidine	[46]
$(Ba_{0.85}Ca_{0.15})(Zr_{0.1}Ti_{0.9})TiO_3$(BCZT)/ Bi_2O_3	Solid-state process	Superior photocatalytic degradation on rhodamine B in UV-vis light	[48]

4. EXPLANATION ON PHOTOCATALYTIC APPLICATIONS OF PZT COMPOSITES

The efficiency of photocatalysts is largely restricted by the rapid recombination of charge carriers in the bulk phase and on the surface of photocatalysts [47]. Polarization has appeared as one of the most important strategies for addressing this issue. The charge separation can be possible by different types of polarization e.g. macroscopic polarization, piezoelectric polarization, ferroelectric polarization and surface

polarization [47]. The strategies and challenges for polarization increment to increase charge separation and photocatalysis are studied by Chen et al [47]. It has been observed on the basis of the nature of chemical bonds, PZT with tetragonal symmetry is very unstable [22]. PZT with tetragonal structure was examined to exhibit ferroelectric properties with high dielectric constant [22]. Because of the development of dipole moment, the cubic structure as shown in Figure 1, is now slightly deformed, with Pb^{2+} and Zr^{4+}/Ti^{4+} ions are displaced relative to the O^{2-} ions, as presented in Fig. 1. The symmetry is now reduced from cubic Pm3m to tetragonal P4mm with c/a=1.0120. The ion displacements destroy the inversion symmetry of the cubic structure and the material is now polar and develops a spontaneous electrical polarization along [001] direction (Fig. 1).

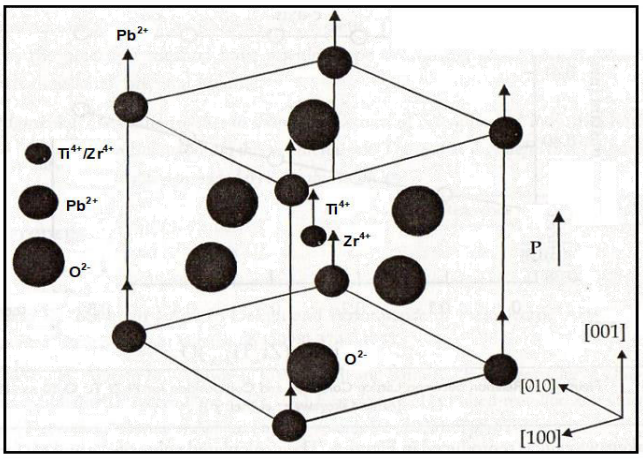

Fig. 1: A tetragonal crystal structure in PZT. The arrow (P) shows the polarization along [001] direction [Adapted from Ref. 22]

Tetragonal phase (P4mm crystal symmetry, with *a* = 0.4036 nm; c=0.4147 nm) was also inferred in addition with the presence of hexagonal symmetry (R3c) with *a* = 0.5774 nm and c = 1.4212 nm, in the as prepared $PbZr_{0.5}Ti_{0.5}O_3$ nanopowders through polymer precursor method [25]. The as prepared $PbZr_{0.5}Ti_{0.5}O_3$ material exhibited specific surface area of $34 m^2/g$. The as synthesized $PbZr_{0.5}Ti_{0.5}O_3$ nanopowder found to exhibit ferroelectric property. The value of ε_{max} was estimated to be 25000 with ε = 1100 at room temperature at 1 kHz. The reduction of Curie temperature, T_C in $PbZr_{0.5}Ti_{0.5}O_3$ nanopowder (T_C = 370°C), in their study, was presumed to be due to the effect of depolarization field [49]. The high value of ε in $PbZr_{0.5}Ti_{0.5}O_3$ nanopowder, in their study, presumed to be probably due to strong surface dipolar interactions in $PbZr_{0.5}Ti_{0.5}O_3$ nanoparticles, as presented in Fig. 2.

The surface dipolar interactions may be the major contributor to the high surface energy of $PbZr_{0.5}Ti_{0.5}O_3$ nanoparticles; one should also consider other effects, such as surface reconstruction and next neighbour interactions etc [50]. Polarization has also been considered by Apostol et al [51] for surface charge generation.

The application of ZnO ceramic piezoelectric nanomaterials in photocatalytic degradation of methylene blue were examined with UV-vis study by Mandal et al [52]. The decrease of peak height in Fig. 3 demonstrates the diminishing concentration of methylene blue with its photocatalytic decomposition with ZnO nanomaterials.

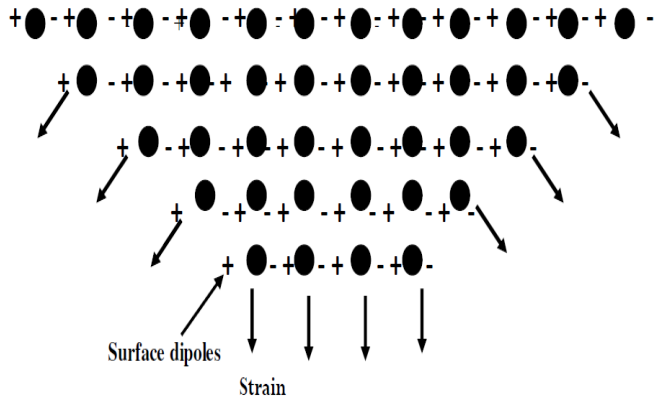

Fig. 2: Schematic view of the surface of a nanoparticle demonstrating the nature of the surface stresses due to inter-dipolar repulsion at the surface [Adapted from Ref. 25]

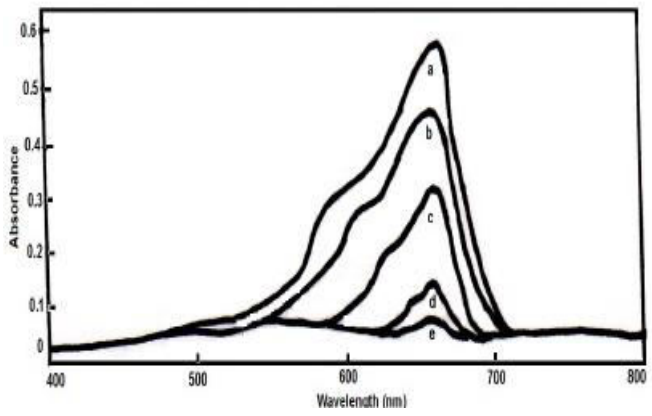

Fig. 3: UV-vis spectra of methylene blue to exhibiting photocatalytic degradation in presence of ZnO nanopowder at (a) starting of the reaction, (b) 1h, (c) 2h, (d) 3h and (e) 4h in presence of sunlight.

5. CONCLUSION

Photocatalytic degradation of organic dyes has been established to be a great method for the environmental protection and the purification of waste water. Ferroelectric PZT based materials are playing a potential role in photodegradation of organic dyes. Unfortunately, the efficiency of environmental remediation and renewable energy generation is seriously restricted by the rapid recombination of charge carriers on the photocatalysts. To overcome this problem Chen et al addressed the strategy of polarization to increase charge separation in order to enhance the photocatalytic efficiency of the as prepared materials. The charge separation can be possible by different types of polarization like piezoelectric polarization, ferroelectric polarization and surface polarization. Recently, Shenyu et al investigated to enhance photodegradation of trimethoxypyrimidine applying piezophotocatalysis of $BaTiO_3/Ag_3PO_4$ exploring mechanical vibration and visible light simultaneously. Abhinay et al found that heterojunction composites of BCZT/Bi_2O_3 exhibited superior photocatalytic activity in compare to BCZT or Bi_2O_3. BCZT/Bi_2O_3 (50:50 ratio) composite showed a lower recombination rate of electron-hole pair and exhibited the maximum photocatalytic performance. Therefore, more studies are required to develop PZT and similar ferroelectric materials for the enhancement of efficiency of photocatalysis for better photocatalytic degradation applications, for the protection of our environment.

6. REFERENCES

1. Ong ST, Keng PS, Lee WN, Ha ST, Hung YT. *Water,* 2011; **3**:157-176.
2. Chen C, Ma W, Zhao J. *Chem. Soc. Rev,* 2010; **39**:4206-4219.
3. Konstantinou IK, Albanis TA. *Appl. Catal. B Environ,* 2004; **49**:1-14.
4. Chowdhury S, Balasubramanian R. *Appl. Catal. B Environ,* 2014; **160-161**:307-324.
5. Qu Y, Duan X. *Chem. Soc. Rev,* 2013; **42**:2568-2580.
6. Chen X, Guo L, Samuel S, Mao SS. *Chem. Rev,* 2010; **110**:6503-6570.
7. Tong H, Ouyang S, Umezawa N, Oshikiri M, Ye J. *Adv. Materials,* 2012; **24(2)**:229-251.
8. Scott JF, Paz de Araujo CA. *Science,* 1989; **246(4936)**:1400-1405.
9. Jaffe H. *The Amer. Ceram. Soc*, 1958; **41(11)**:494-498.
10. Yang WC, Rodriguez BJ, Gruverman A, Nemanich RJ. *J. Phys. Condens. Matte,* 2005; **17**:1415-1426.
11. Giocondi JL, Rohrer GS. *Chem. Mater,* 2001; **13**:241-242.
12. Giocondi JL, Rohrer GS. *J. Phys. Chem. B,* 2001; **105**:8275-8277.
13. Dunn S, Jones PM, Gallardo DE. *J. Am. Chem. Soc,* 2007; **129**:8724-8728.
14. Kalinin SV, Bonnell DA, Alvarez T, et al. *Nano Lett.,* 2002; **2**:589-593.
15. Cabrera AL, Vargas F, Albers JJ. *Surf. Sci.,* 1995; **336**:280 -286.
16. Cabrera AL, Vargas F, Zarate RA. *J. Phys. Chem. Solids,* 1994; **55**:1303-1307.
17. Uchino K. *Acta Mater.,* 1998; **46(11)**:3745-3753.
18. Mandal TK, Ram S. *Mater. Lett.,* 2003; **57(16-17)**:2432 - 2442.
19. Ram S, Mandal TK. *J. Mater. Sci. Lett.,* 2003; **22**:675-678.
20. Mandal TK, Ram S, Kundu TK. *Ind. J. Phys.,* 2004; **78A**:233-237.
21. Ram S, Mandal TK. *Journal of the American Ceramic Society,* 2005; **88**:3444-3448.
22. Mandal TK. *The ICFAI Journal of Science and Technology,* 2005; **1**:39-45.
23. Mandal TK. *Appl. Phys. Lett.,* 2006; **89**:034103(1-3).
24. Mandal TK. *Indian J Physics,* 2012; **86**:818-888.
25. Mandal TK. *Materials Science Poland,* 2015; **33**:18-24.
26. Misri I, Hareesh P, Yang SY, Devoe DL. *J. Micromech. Microeng.*, 2012; **22**:085017.
27. Srivastavan G, Goswami Ankur, Umarji AM. *Ceram. International,* 2013; **39**:1977.
28. Ragini, Mishra SK, Pandey D. *Phys. Rev. B.,* 2001; **64**:054101.
29. Zeng J, Song S, Wang L, Zhang MZ, Zheng L, Lin C. *J. Am. Ceram. Soc*., 1999; **82**:461.
30. Wu A, Vilarinho PM, Salvado IMM, Bapista JL. *J. Am. Ceram. Soc.,* 2000; **83**:1379.
31. Sorowiak Z, Kupriyanov MF, Czekaj DJ. *J. Euro. Ceram. Soc.,* 2001; **21**:1377.
32. James AR, Kumar Rajesh, Kumar Prem, Srinivas MK, Radha V, Vithal M, Vijayakumar M. *Journal of Alloys and Compounds*, 2010; **496**:624-627.
33. Peng JH, Hojamberdiev M, Li HQ, Mao DL, Zhao YJ, Liu P, Zhou JP, Zhu GQ. *Journal of Magnetism and Magnetic Materials,* 2015; **378**:298-305.

34. Wang J, Trodahl J, Sandu C, Gregora I, Setter N. *Journal of the European Ceramic Society,* 2014; **34**:2311-2316.
35. Wu CG, Sun XY, Meng J, Luo WB, Li P, Peng QX, et al. *Infrared Physics & Technology,* 2014; **63**:69-73.
36. Bortolani F, Dorey RA. *Journal of the European Ceramic Society,* 2010; **30**:2017-2079.
37. Schneller T, Waser R. *Journal of Sol-Gel Science and Technology*, 2007; **42**:337-352.
38. Wu Q, Li D, Wu L, Wang J, Fu X, Wang X. *J. Mater. Chem.*, 2006; **16**:1116-1117.
39. Huang H , Li D, Lin Q, Shao Y, Chen W, Hu Y, Chen Y, Fu X. *J. Phys. Chem. C.,* 2009; **113(32)**:14264-14269.
40. Lai CW, Samsudin EM, Juan JC. *Advanced Materials Research,* 2015; **1087**:186-190.
41. You H, Wu Z, Jia Y, Xu X, Xia Y, Han Z, Wang Y. *Chemosphere*, 2017; **183**:528-535.
42. Liang Z, Yan CF, Rtimi S, Bandara J. *Applied Catalysis B: Environmental,* 2018; **241**.
43. Feng Y, Li H, Ling L, Yan S, Pan D, Ge H, et al. *Environ Sci Technol.,* 2018; **52(14)**:7842-7848.
44. Qifeng L, Jingjun M, Sharma M, Vaish R. *J. American Ceramic Society,* 2019; **102(10)**:5807-5817.
45. Shuya X, Zhihong L, Maolin Z, Limin G. *Journal of Alloys and Compounds,* 2019; **801**:483-488.
46. Shenyu L, Xiangkang Z, Rayees AR, Irene M, Chi L. *Environmental Science: Nano,* 2019; **6**:554-564.
47. Chen F, Huang H, Guo L, Zhang Y, Ma T. *Angewandte Chemie International Edition,* 2019; **58(30)**:10061-10073.
48. Abhinay S, Tarai P, Mazumder R. *Journal of Materials Science,* 2020; **55(5)**:1904 - 1914.
49. Begg BD, Vance ER, Nowotny J. *J. Am. Ceram. Soc.,* 1994; **77(12)**:3186-3192.
50. Ayyub P. *Phys. Edun.,* 1998; **Jan-March**: 309.
51. Apostol NG, Husanu MA, Lizzit D, Hristea IA, Chirilă CF, Trupină L, Teodorescu CM. *Catalysis Today,* 2021; **366**:141-154.
52. Mandal TK, Malhotra SPK, Singh RK. *Romanian Journal of Materials,* 2018; **48(1)**:32-38.